

Blends of Poly[3,3-bis(Chloromethyl)Oxetane] with Poly(vinyl Acetate). I. Thermal and Mechanical Properties

LIU WEILIAN, GUO QIPENG* and FENG ZHILIU

Laboratory of Polymer Physics, Changchun Institute of Applied Chemistry, Academia Sinica, Changchun 130022, China

SYNOPSIS

Blends of poly[3,3-bis(chloromethyl)oxetane] (Penton) with poly(vinyl acetate) were prepared. Compatibility, morphology, thermal behavior, and mechanical properties of blends with various compositions were studied using differential scanning calorimetry (DSC), dynamic mechanical measurements (DMA), tensile tests, and scanning electron microscopy (SEM). DMA study showed that the blends have two glass transition temperatures (T_g). The T_g of the PVAc rich phase shifts significantly to lower temperatures with increasing Penton content, suggesting that a considerable amount of Penton dissolves in the PVAc rich phase, but that the Penton rich phase contains little PVAc. The Penton/PVAc blends are partially compatible. DSC results suggest that PVAc can act as a β -nucleator for Penton in the blend. Marked negative deviations from simple additivity were observed for the tensile strength at break over the entire composition range. The Young's modulus curve appeared to be S-shaped, implying that the blends are heterogeneous and have a two-phase structure. This was confirmed by SEM observations. © 1992 John Wiley & Sons, Inc.

INTRODUCTION

Poly[3,3-bis(chloromethyl)oxetane] (Penton) is a light-colored, semicrystalline thermoplastic. Its high chlorine content of 45.5 wt % makes the polymer self-extinguishing. The high chlorine content, the fact that the chlorine atoms are of the neopentyl type and therefore resistant to dehydrochlorination, and the high degree of crystallinity impart to the polymer a high degree of chemical resistance, even at moderately high temperatures.¹ However, only a few studies have been done on blends of Penton with other polymers, which involve the miscibility and properties of Penton/poly(ϵ -caprolactone) blends.^{2,3}

This article presents the results of our work on blends of Penton and poly(vinyl acetate) (PVAc). Attention was paid to the compatibility and thermal and mechanical properties of these blends. Dynamic mechanical measurements (DMA), differential scanning calorimetry (DSC), tensile tests, and

scanning electron microscopy (SEM) were used for analyses.

EXPERIMENTAL

Materials and Preparation of Blends

Penton and PVAc were supplied by Shanghai Synthetic Resins Co. (China) with a quoted average mol wt of 350,000 and 30,000, respectively. Penton/PVAc blends, with weight ratios of 100/0, 90/10, 80/20, 60/40, 40/60, 20/80, and 0/100, were prepared by a Brabender at 180°C for 15 min. The samples were further pressed at 180°C into sheets.

Differential Scanning Calorimetry

A Perkin-Elmer, DSC-7 differential scanning calorimeter was employed to study the melting behavior of the samples. The sample weight used in the DSC cell was kept in the range 8 to 12 mg. The samples were first heated to 200°C to remove prior thermal histories. They were then cooled to 50°C at a rate of 20°C/min to trace the crystallization process,

* To whom correspondence should be addressed.

followed by heating to 200°C again at a heating rate of 20°C/min to observe the melting behavior. The heat of fusion was calculated from the melting peak area; the maximum of the endotherm and the minimum of the exotherm were taken as the melting temperature (T_m) and the crystallization temperature (T_c), respectively.

Dynamic Mechanical Measurements

Dynamic mechanical measurements were carried out on a Rheovibron Model DDV-II-EA dynamic viscoelastometer (Toyo Baldwin Co., Japan). The frequency used was 3.5 Hz and the heating rate was 3.0°C/min. Specimen dimension was 4.0 × 0.4 × 0.03 cm.

Tensile Tests

Tensile tests were carried out on an Instron Model 1122 testing machine at room temperature. Standard dumbbell specimens with a 2 × 0.40 × 0.05 cm neck were used. Average values were obtained from five

to ten successful determinations. Crosshead speed was 2.0 cm/min, corresponding to a relative strain rate of 1.0 min⁻¹.

Observation of Morphology

A JEOL JXA-840 scanning electron microscope (SEM) was used to observe the fracture surfaces of the specimens, which were coated with a thin layer of platinum of about 200 Å.

RESULTS AND DISCUSSION

Glass Transition Temperature

Tan δ vs. T curves of Penton, PVAc, and their blends are shown in Figure 1. The abrupt increases of tan δ to around 180°C for pure Penton and the blends are attributable to the melting of the crystalline phases of Penton. For pure Penton, the tan δ vs. T curve shows a relaxation peak at 15°C, which is due to its glass transition. For pure PVAc, the maximum

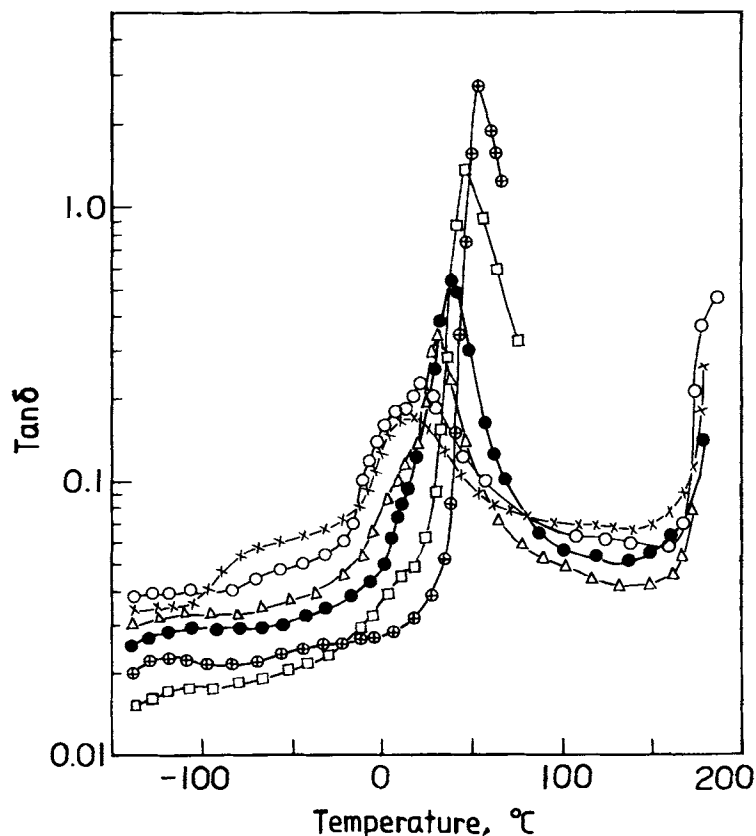


Figure 1 Temperature dependence of tan δ of Penton/PVAc blends with compositions (\times) 100/0, (O) 80/20, (Δ) 60/40, (\bullet) 40/60, (\square) 20/80, and (\oplus) 0/100.

at ca. 50°C of the $\tan \delta$ vs. T curve corresponds to its T_g . This maximum shifts to low temperatures with increasing Penton content in the blend. It can also be seen that there exists a shoulder at the low temperature side of the $\tan \delta$ vs. T curves, responsible for the T_g of the Penton rich phase. The T_g data obtained from Figure 1 are listed in Table I and are plotted in Figure 2 as a function of blend composition. The fact that the T_g of the PVAc rich phase shifts to lower temperature with an increase in Penton content suggests that a considerable amount of Penton was dissolved in the PVAc rich phase. The T_g values of the Penton rich phase are roughly estimated from the shoulder. They only vary within a few degrees with blend composition, implying that the Penton rich phase contains little PVAc. These results suggest that the Penton/PVAc blends are partially compatible.

Cooling Crystallization and Melting Behavior

Figure 3 shows the DSC traces of Penton and the blends at a cooling rate of 20°C/min from 200°C. The related cooling crystallization data are listed in Table II. For the pure Penton, an exothermic peak occurs at $T_c 1 = 118^\circ\text{C}$. For the 90/10 Penton/PVAc blend, $T_c 1$, is 106°C, which is 12°C lower than that of pure Penton, indicating that the crystallization rate of Penton in the blend becomes much slower. However, the blend's $T_c 1$ increases with increasing PVAc content when the PVAc content is higher than 10 wt %. Furthermore, for the blends with PVAc content of 40 wt % or more, there appears a shoulder $T_c 2$ at the left side of the $T_c 1$ peak, due to the formation of the β -crystalline form of Penton. Figure 4 summarizes the values of $T_c 1$ and $T_c 2$ as functions of blend composition. It can also be clearly seen that the crystallization temperature, $T_c 1$, of Penton shows a minimum at 10 wt % PVAc, then gradually

Table I T_g Values of Penton/PVAc Blends Obtained by DMA

Penton/PVAc (w/w)	T_g (Penton) (°C)	T_g (PVAc) (°C)
100/0	15	—
90/10	16	25
80/20	10	22
60/40	18	31
40/60	13	40
20/80	12	46
0/100	—	52

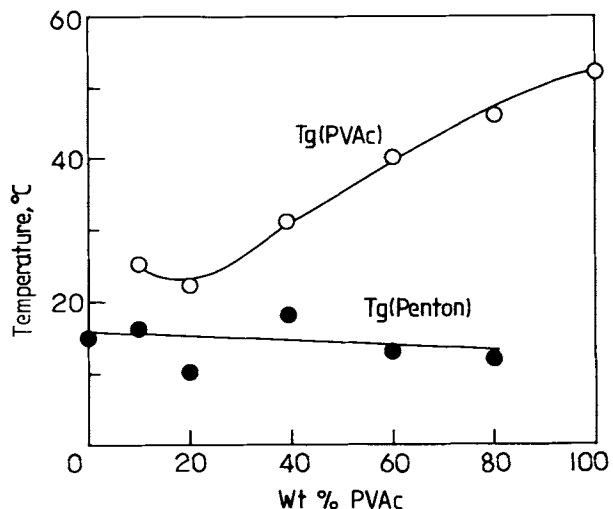


Figure 2 Glass transition behavior for Penton/PVAc blends.

increases with PVAc content. The initial decrease in $T_c 1$ can be attributed to the limited dissolution of PVAc in Penton. The increase in $T_c 1$ beyond 10 wt % is due to the nucleation effect of the separated PVAc phase. The appearance of $T_c 2$, and the fact that its value increases with PVAc content, suggest that PVAc can act as a β -nucleator for Penton in the blend.

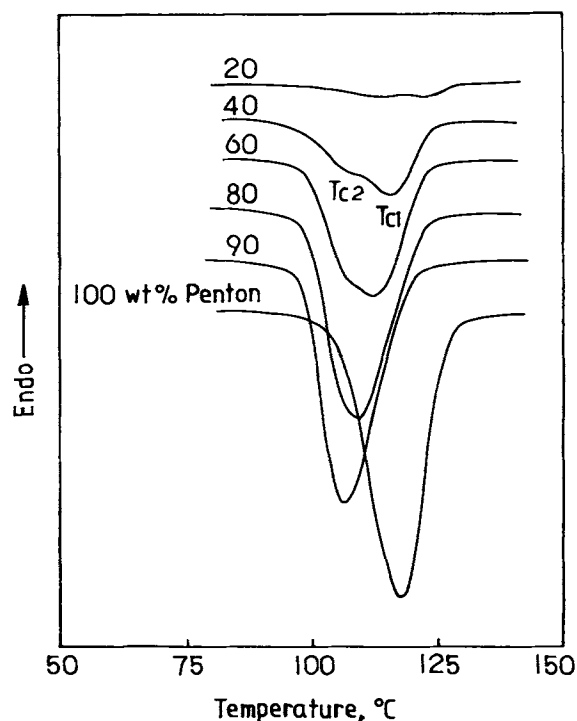


Figure 3 Crystallization curves of Penton/PVAc blends during the cooling at 20°C/min.

Table II Cooling Crystallization Data of Penton/PVAc Blends

Penton/PVAc (w/w)	ΔH_c		T_{c1} (°C)	T_{c2} (°C)
	(J/g Blend)	(J/g Penton)		
100/0	-34.5	-34.5	118	—
90/10	-30.7	-34.1	106	—
80/20	-28.4	-35.5	109	—
60/40	-21.1	-35.2	112	108
40/60	-12.2	-30.5	116	108
20/80	-2.7	-13.5	123	114
0/100	—	—	—	—

The melting behavior after the cooling from the melt for the Penton and the blends is presented in Figure 5. In Table III are listed the melting temperatures and endothermic heats of pure Penton and its blends. It can be seen that the pure Penton exhibits two melting endothermic peaks, T_{m1} and T_{m3} , referring to the melting of its β - and α -crystalline forms, respectively. For the blends, a new endothermic peak, T_{m2} , appears between T_{m1} and T_{m3} . T_{m3} is due to the melting of the α -form of Penton, while both T_{m1} and T_{m2} can be attributed to the β -form.⁴⁻⁶ Sandiford⁴ has observed that the β -form occurs when the quenched amorphous Penton is crystallized by heating at a temperature above its glass transition temperature. It also occurs by crystallizing from the melt under pressure.⁵ In the present case, the double melting phenomenon of the β -phase itself, during DSC measurements, may be

caused by melting of the original β -phase formed during the cooling, and subsequent recrystallization during the heating to β -form and its melting. Plots of the T_m s vs. blend composition in Figure 6 show that all the values do not decrease with increase of PVAc content. Actually, they slightly increase with PVAc content. This is in accordance with the result that the Penton/PVAc blends are not completely compatible.

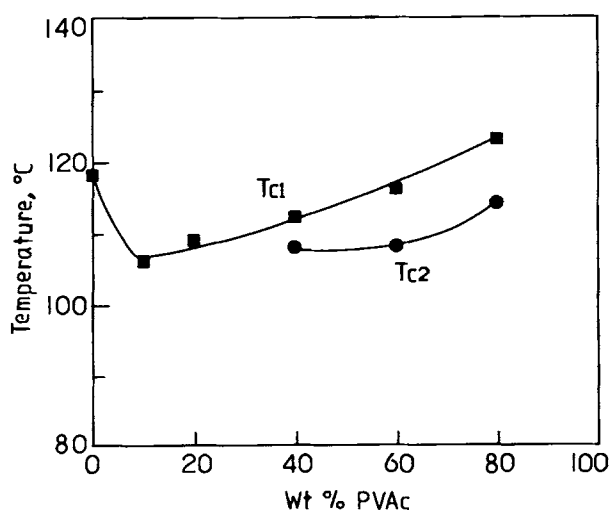
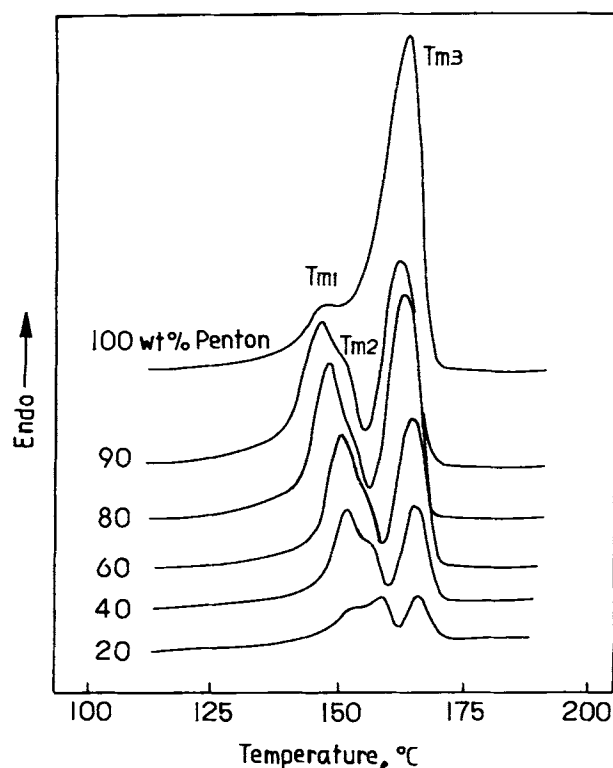
**Figure 4** Composition dependence of nonisothermal crystallization temperatures of Penton/PVAc blends.**Figure 5** DSC curves of Penton/PVAc blends after the cooling crystallization. The heating rate is 20°C/min.

Table III Melting Behavior of Penton/PVAc Blends

Penton/PVAc (w/w)	ΔH_f (Total)		T_{m1}/T_{m2} (°C)	T_{m3} (°C)
	(J/g Blend)	(J/g Penton)		
100/0	36.0	36.0	148/—	165
90/10	33.0	36.7	147/151	163
80/20	30.0	37.5	149/153	164
60/40	22.6	37.7	152/155	166
40/60	14.8	37.0	152/157	166
20/80	8.0	40.0	154/159	167
0/100	—	—	—	—

Tensile Properties

No obvious yield was observed on the stress-strain curves, which shows that Penton, PVAc, and their blends were basically brittle materials at the strain rate of 1.0 min^{-1} and room temperature. However, the stress-strain curve of pure Penton exhibited some characteristics of ductile fracture. From the initial slopes, Young's moduli of Penton, PVAc, and their blends were calculated. In Figure 7, the Young's modulus is plotted as a function of blend composition. It can be seen that, first, the Young's modulus increases with increasing PVAc content. Second, the Young's modulus curve is S-shaped. This fact implies that the blends are heterogeneous and have a two-phase structure.

The properties at high deformation are illustrated in Figures 8 and 9 by their tensile strength and elongation at break, respectively. Marked negative deviation from simple additivity is observed for the tensile strength at break over the entire composition range, which is typical for an essentially incompatible system.⁷⁻¹¹ It may be reasonable to conclude that interfaces between Penton and PVAc are weakly bounded with poor interaction. However, the elongation at break of the blends does not show negative deviation. It is interesting to see that marked positive deviations are observed at some compositions.

In Figure 10, fractographs of the two samples of Penton/PVAc blends (80/20 and 20/80) clearly show a two-phase structure of the blend and the poor adhesion between phases. For the 80/20 Penton/PVAc blend, PVAc was well dispersed in the

gation at break, respectively. Marked negative deviation from simple additivity is observed for the tensile strength at break over the entire composition range, which is typical for an essentially incompatible system.⁷⁻¹¹ It may be reasonable to conclude that interfaces between Penton and PVAc are weakly bounded with poor interaction. However, the elongation at break of the blends does not show negative deviation. It is interesting to see that marked positive deviations are observed at some compositions.

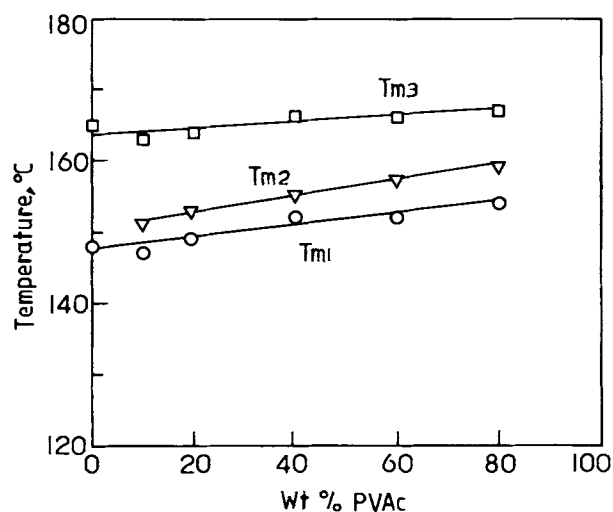


Figure 6 Variation of the melting temperatures of Penton/PVAc blends with composition.

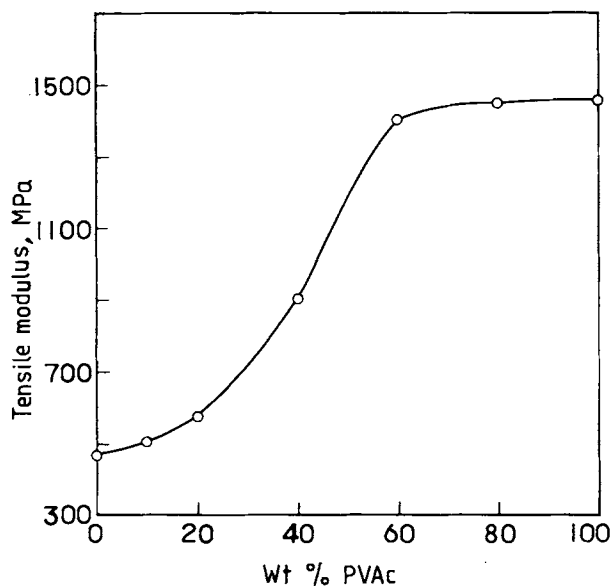


Figure 7 Composition dependence of tensile modulus at room temperature (20°C) for Penton/PVAc blends.

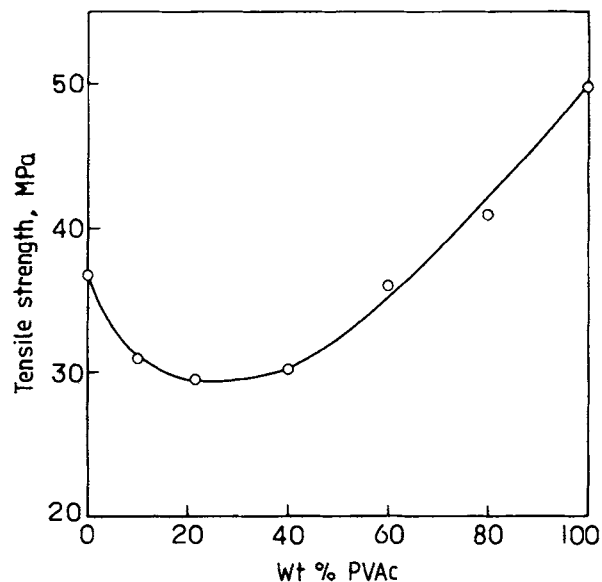


Figure 8 Composition dependence of tensile strength at room temperature (20°C) for Penton/PVAc blends.

continuous Penton phase [Fig. 10(a)]. It can be seen that the fracture occurred in a macroscopically brittle manner, but with a little evidence of ductility in the Penton continuous phase. For the 20/80 Penton/PVAc blend, well defined domains of Penton were dispersed in a continuous PVAc phase; the fractured surface shows the characteristics of brittle fracture [Fig. 10(b)].

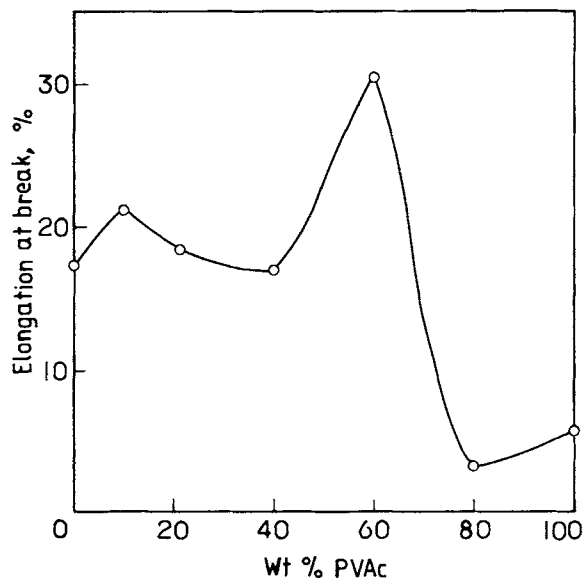


Figure 9 Composition dependence of elongation at break at room temperature (20°C) for Penton/PVAc blends.

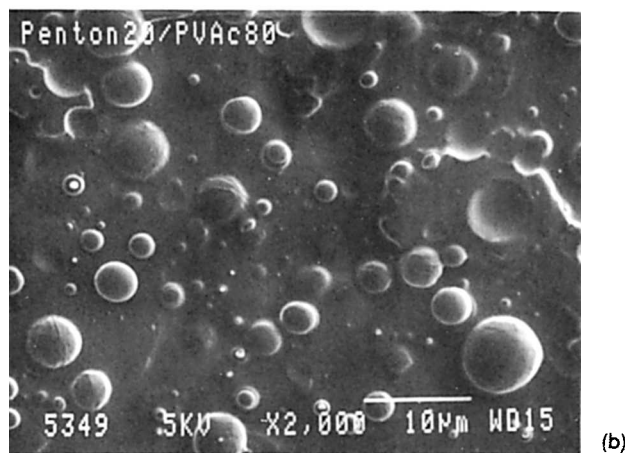
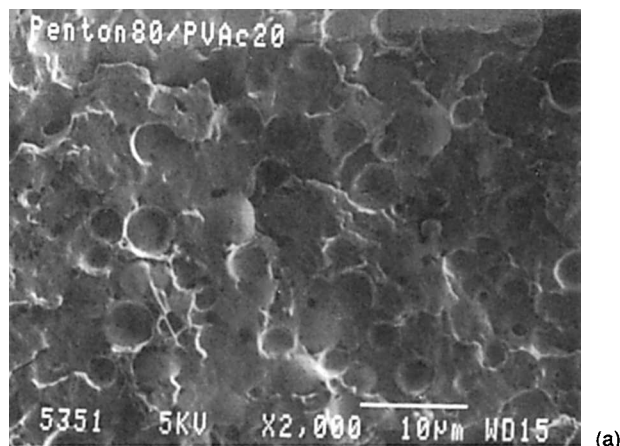


Figure 10 Scanning electron micrographs of fractured surfaces of (a) 80/20 and (b) 20/80 Penton/PVAc blends.

CONCLUSIONS

The results presented in this article show that Penton and PVAc are partially compatible. Their blends have two T_g s, corresponding to those of the Penton and PVAc rich phases, respectively. The lowering of T_g of the PVAc rich phase with increasing Penton content suggests that a considerable amount of Penton dissolves in the PVAc rich phase, while the Penton rich phase contains little PVAc. DSC study shows that PVAc can act as a β -nucleator for Penton in the blend. Marked negative deviations from simple additivity are observed for the tensile strength at break over the entire composition range, as expected for an essentially incompatible system. The Young's modulus curve appears S-shaped. SEM observations reveal that the blends have a two-phase structure, which supports the other results well.

This work was partly supported by the National Natural Science Foundation of China.

REFERENCES

1. H. Boardman, in: *Ency. Polym. Sci. Eng.*, Vol. 9, H. F. Mark, Ed., John Wiley & Sons, Inc., New York, p. 702.
2. J. V. Koleske, in: *Polymer Blends*, Vol. 2, D. R. Paul and S. Newman, Eds., Academic, New York, 1978, Chap. 22.
3. Q. Guo, *Makromol. Chem.*, **191**, 2639 (1990).
4. D. J. H. Sandiford, *J. Appl. Chem.*, **8**, 188 (1958).
5. J. R. Collier and E. Baer, *Technical Report 19, Polymer Science & Engineering*, Case Institute of Technology, Cleveland, OH, Jan. 14, 1966.
6. I. Kazuyoski and K. Shoichi, *J. Appl. Polym. Sci.*, **6**, S52 (1962).
7. J. Kohler, G. Riess, and A. Banderet, *Eur. Polym. J.*, **4**, 173, 187 (1968).
8. E. H. Merz, G. C. Claver, and M. Baer, *J. Polym. Sci.*, **22**, 325 (1956).
9. J. Periard, A. Banderet, and G. Riess, *Angew. Makromol. Chem.*, **15**, 31, 35 (1971).
10. P. Bataille, S. Boisse, and H. P. Schreiber, *Polym. Eng. Sci.*, **27**, 622 (1987).
11. J. Huang, B. Jiang, and Q. Guo, *Eur. Polym. J.*, **26**, 61 (1990).

Received May 20, 1991

Accepted January 8, 1992